Inorg. Chem. **2006**, *45*, 10230–10239

Synthesis and Vibrational Circular Dichroism of Enantiopure Chiral Oxorhenium(V) Complexes Containing the Hydrotris(1-pyrazolyl)borate Ligand

Peter R. Lassen,[†,‡] Laure Guy,[§] Iyad Karame,[§] Thierry Roisnel,[||] Nicolas Vanthuyne,[⊥] Christian Roussel,[⊥] Xiaolin Cao,[†] Rosina Lombardi,[†] Jeanne Crassous,*[,||] Teresa B. Freedman,*[,†] and Laurence A. Nafie[†]

Department of Chemistry, Syracuse University, Syracuse, New York 13244, Laboratoire de Chimie, École Normale Supérieure de Lyon, UMR CNRS 5182, 46 Allée d'Italie, F-69364 Lyon 07, France, Sciences chimiques de Rennes, UMR CNRS 6226, Université de Rennes 1, Campus de Beaulieu, 35042 Rennes Cedex, France, and UMR Chirotechnologies: Catalyse et Biocatalyse, Université Paul Cézanne, 13397 Marseille Cedex 20, France

Received July 28, 2006

The infrared and vibrational circular dichroism (VCD) spectra of six chiral oxorhenium(V) complexes, bearing a hydrotris(1-pyrazolyl)borate (Tp) ligand, have been investigated. These complexes are promising candidates for observation of parity violation (symmetry breaking due to the weak nuclear force). New chiral oxorhenium complexes have been synthesized, namely, [TpReO(η^2-O(CH_3)CH_2CH_2O-*O*,*O*)] (**4a** and **4b**) diastereomers and [TpReO(η^2-N(CH_3)CH_2CH_2O-*N*,*O*)] (**5**) and [TpReO(η^2-N(*t*Bu)CH_2CH_2O-*N*,*O*)] (**6**) enantiomers. All compounds could be obtained in enantiomerically pure form by using either column chromatography or HPLC over chiral columns. VCD spectroscopy of these compounds and of [TpReO(η^2-N(CH_3)CH(CH_3)CH(Ph)O-*N*,*O*)] (**2**) and [TpReO(η^2-N(CH_2)$_3$$CHCO_2$-*N*,*O*)] (**3**) (with chiral bidentate ligands derived, respectively, from ephedrine and proline) were studied. This allowed the absolute configuration determination of all compounds together with their conformational analysis, by comparing calculated and experimental spectra. This is the first VCD study of rhenium complexes which further demonstrates the applicability of VCD spectroscopy in determining the chirality of inorganic complexes.

Introduction

Oxorhenium complexes have proven useful in catalysis[1] and in radiopharmaceutical chemistry.[2] Moreover, chiral oxorhenium complexes have been revealed to be good candidates for the observation of parity violation (PV) effects in chiral molecules.[3] Parity violation is a fundamental effect which breaks the space symmetry and which is due to weak interaction between elementary particles.[4] It has been experimentally observed in atoms and in nuclear physics.[5] At the molecular level, PV is known to induce a very tiny energy difference (PVED) between the two enantiomers of a chiral molecule. However, observing such a tiny energy difference, ΔE_{PV} (ΔE_{PV} = ca. 10^{-17} kT) is still a scientific challenge and requires very accurate spectroscopy methods together with a good chiral model molecule.[6] For example, PV may be observed by unpolarized infrared (IR) spectroscopy, i.e., by measuring slightly different absorption frequencies for opposite enantiomers. PVED measurements have already been searched on simple chiral heterohalogenomethanes such

* To whom correspondence should be addressed. (J.C.) Phone: +33 02 23 23 63 70. Fax: +33 02 23 23 69 39. E-mail: jeanne.crassous@univ-rennes1.fr. (T.B.F.) Phone: (315) 443-1134. Fax: (315) 443-4070. E-mail: tbfreedm@syr.edu.

[†] Syracuse University.

[‡] Visiting from the Quantum Protein Centre, Department of Physics, Technical University of Denmark, DK-2800 Lyngby, Denmark.

[§] École Normale Supérieure de Lyon.

[||] Université de Rennes 1.

[⊥] Université Paul Cézanne.

(1) (a) Morris, L. J.; Downs, A. J.; Greene, T. M.; McGrady, G. S.; Herrmann, W. A.; Sirsch, P.; Scherer, W.; Gropen, O. *Organometallics* **2001**, *20*, 2344−2352 and references therein. (b) Kennedy-Smith, J. J.; Nolin, K. A.; Gunterman, H. P.; Toste, F. D. *J. Am. Chem. Soc.* **2003**, *125*, 4056−4057. (c) Morrill, C.; Grubbs, R. H. *J. Am. Chem. Soc.* **2005**, *127*, 2842−2843. (d) Rudolph, J.; Reddy, K. L.; Chiang, J. P.; Sharpless, K. B. *J. Am. Chem. Soc.* **1997**, *119*, 6189−6190. (e) Cai, Y.; Espenson, J. H. *Inorg. Chem.* **2005**, *44*, 2560−2565. (f) Ison, E. A.; Trivedi, E. R.; Corbin, R. A.; Abu-Omar, M. M. *J. Am. Chem. Soc.* **2005**, *127*, 15374−15375.

10.1021/ic061418m CCC: $33.50
Published on Web 11/08/2006

as CHFClBr, resulting in the determination of an experimental upper limit of 10 Hz for this effect.[7] Meanwhile, theoreticians have shown that transition-metal complexes such as rhenium compounds, i.e., bearing a heavy metal[3,8] near the chirality center, are very promising compounds. Indeed, they display much higher PV effects than organic compounds, thanks to the dependence of ΔE_{PV} on the nuclear charge of the atoms in the molecule; this difference (ΔE_{PV}) scales approximately like Z^5.[9,10]

Oxorhenium complexes usually display a sharp Re═O stretching mode around 950 cm^{-1}. We have found a number of chiral oxorhenium complexes in the literature[11] and have focused our attention on enantiomerically pure Faller's oxorhenium complexes containing a hydrotris(1-pyrazolyl)-borate (Tp) ligand because they are readily available, robust, and "chiral at the rhenium".[11b] In this context, we show in this paper that VCD spectroscopy is a valuable tool for finding the best candidate molecule which displays all the features for PV experiments. The VCD spectrum of the bulk solution provides important information on whether the Re═O stretching absorption band is active or not, on the absolute configuration of the sample, and on the conformers present in solution.

VCD spectroscopy is an advanced form of IR absorption spectroscopy, in which information about the chirality of a sample is obtained by the differential absorption of left and right circularly polarized IR radiation.[12] Compared to those of electronic circular dichroism, VCD spectra are more detailed because of the many bands contained in the mid-IR "fingerprint" region. Since the discovery of VCD three decades ago,[13] the technique has been applied mostly to small organic molecules. Commercial software for calculations of VCD spectra was introduced in 1998, allowing direct comparison with experimental data. Recently, VCD has been calculated for several transition-metal complexes and successfully compared to experiments.[14]

In this paper we present the synthesis and the separation of enantiomerically pure new compounds (R_{Re}*,R_C*)- and (R_{Re}*,S_C*)-[TpReO(η^2-O(CH_3)CH_2CH_2O-*O*,*O*)] (**4a** and **4b**, respectively) (four stereoisomers), together with (R_{Re})- and (S_{Re})-[TpReO(η^2-N(CH_3)CH_2CH_2O-*N*,*O*)] (**5**) and (R_{Re})- and (S_{Re})-[TpReO(η^2-N(*t*Bu)CH_2CH_2O-*N*,*O*)] (**6**), where Tp = hydrotris(1-pyrazolyl)borate (see Schemes 1 and 2). Analytical and semipreparative HPLC over chiral columns of **5** and **6** enantiomers has been performed. A benchmark analysis of chiral oxorhenium complexes is presented in detail, which includes IR and VCD spectra of the compounds along with the density functional theory (DFT) calculated ones. In the first step, the calculation methods (choice of the basis sets and of the density functional) have been determined on already known complexes (R_{Re},R_{O-C},S_{C-N})-(+)-**2** and (R_{Re},R_C)-(−)-**3**. In the second step, the comparison of experimental and calculated VCD spectra allowed the determination of the (R_{Re},R_C)-(+)-**4a**, (R_{Re},S_C)-(−)-**4b**, (R_{Re})-(−)-**5**, and (R_{Re})-(−)-**6** absolute configurations. X-ray crystallography enabled confirmation of the absolute configurations for **4a** and **4b** (see Figure 1). In the case of compounds **3**, **4b**, and **5**, VCD studies showed the presence of several conformers in solution. These are important features for the choice of the best candidate for future PV measurements by IR spectroscopy.

Results and Discussion

Synthesis and Separation of Compounds. The samples studied first were the two enantiomeric pairs (S_{Re},S_{O-C},R_{C-N})- and (R_{Re},R_{O-C},S_{C-N})-[TpReO(η^2-N(CH_3)CH(CH_3)CH(Ph)O-

(2) (a) Nicolini, A.; Bandoli, G.; Mazzi, U. *Technetium, Rhenium and Other Metals in Chemistry and Nuclear Medicine, 5*; Raven Press: New York, 2000. (b) Liu, S. *Chem. Soc. Rev.* **2004**, *33*, 445−461. (c) Jurisson, S. S.; Lydon, J. D. *Chem. Rev.* **1999**, *99*, 2205−2218.
(3) Schwerdtfeger, P.; Bast, R. *J. Am. Chem. Soc.* **2004**, *126*, 1652−1653.
(4) Quack, M. *Angew. Chem., Int. Ed.* **2002**, *41*, 4618−4630 and references therein.
(5) (a) Bouchiat M. A.; Bouchiat, C. C. *Phys. Lett.* **1974**, *48B*, 111−114. (b) Barkov, L. M.; Zolotorev, M. S. *JETP* **1980**, *52*, 360−376. (c) Bouchiat, M. A.; Bouchiat, C. C. *Rep. Prog. Phys.* **1997**, *60*, 1351−1396. (d) Wood, C. S.; Bennett, S. C.; Cho, D.; Masterson, B. P.; Roberts, J. L.; Tanner, C. E.; Wieman, C. E. *Science* **1997**, *275* (5307), 1759−1763. (e) Wu, C. S.; Ambler, E.; Hayward, R.; Hoppes, W. D. D.; Hudson, R. P. *Phys. Rev.* **1957**, *105*, 1413−1415.
(6) (a) Crassous, J.; Chardonnet, C.; Saue, T.; Schwerdtfeger, P. *Org. Biomol. Chem*. **2005**, *3*, 2218−2224. (b) Crassous, J.; Monier, F.; Dutasta, J. P.; Ziskind, M.; Daussy, C.; Grain, C.; Chardonnet, C. *ChemPhysChem* **2003**, *4*, 541−548.
(7) (a) Daussy, C.; Marrel, T.; Amy-Klein, A.; Nguyen, C. T.; Bordé, C. J.; Chardonnet, C. *Phys. Rev. Lett.* **1999**, *83*, 1554−1557. (b) Chardonnet, C.; Daussy, C.; Marrel, T.; Amy-Klein, A.; Nguyen, C. T.; Bordé, C. J. In *Parity violation in atomic physics and electron scattering*; Frois, B., Bouchiat, M. A., Eds.; World Scientific: New York, 1999; pp 325−355. (c) Chardonnet, C.; Marrel, T.; Ziskind, M.; Daussy, C.; Amy-Klein, A.; Bordé, C. J. *J. Phys. IV* **2000**, *10-Pr8*, 45−54. (d) Shelkovnikov, A.; Grain, C.; Butcher, R. J.; Amy-Klein, A.; Goncharov, A.; Chardonnet, C. *IEEE J. Quantum Electron.* **2004**, *40*, 1023−1029.
(8) (a) Schwerdtfeger, P.; Gierlich, J.; Bollwein, T. *Angew. Chem., Int. Ed*. **2003**, *42*, 1293−1296. (b) Laerdahl, J. K.; Schwerdtfeger, P.; Quiney, H. M. *Phys. Rev. Lett.* **2000**, *84*, 3811−3814.
(9) Schwerdtfeger, P.; Saue, T.; van Stralen, J. N. P.; Visscher, L. *Phys. Rev. A* **2005**, *71*, 012103−1−7.
(10) Finding the ideal chiral candidate molecule for the first observation of parity violation at the molecular level is a real challenge. The design of the best candidate is related to the ultra-high-resolution spectroscopy technique involved in the measurement. The experimental and theoretical aspects of the PV measurement impose several requirements such as (i) a very simple molecule with the total number of atoms as few as possible, (ii) a heavy atom such as rhenium near the chiral center, (iii) a rigid molecule for good spectroscopic properties, and (iv) an isolated absorption peak with a frequency lying in the domain 1000 ± 100 cm^{-1} which is imposed by the use of an ultrastable CO_2 laser in the case of ultra-high-resolution IR spectroscopy (see refs 6 and 7).
(11) (a) Nolin, K. A.; Ahn, R. W.; Toste, F. D. *J. Am. Chem. Soc.* **2005**, *127*, 12462−12463. (b) Faller, J. W.; Lavoie, A. R. *Organometallics* **2000**, *19*, 3957−3962. (c) Parr, M. L.; Perez-Acosta, C.; Faller. J. W. *New J. Chem.* **2005**, *29*, 613−619. (d) Rybak, W. K.; Sharzynska, A.; Glowiak, T. *Angew. Chem., Int. Ed.* **2003**, *42*, 1725−1727. (e) Rybak, W. K.; Sharzynska, A.; Szterenberg, L.; Ciunik, Z.; Glowiak, T. *Eur. J. Inorg. Chem.* **2005**, 4964−4975. (f) Hansen, L.; Yue, K. T.; Xu, X.; Lipowska, M.; Taylor, A., Jr.; Marzilli, L. G. *J. Am. Chem. Soc.* **1997**, *119*, 8965−8972. (g) Herrmann, W. A.; Marz, D. W.; Herdtweck, E. *J. Organomet. Chem.* **1990**, *394*, 285−303. (h) Tessier, C.; Rochon, F. D.; Beauchamp, A. L. *Inorg. Chem.* **2002**, *41*, 6527−6536. (i) Melian, C.; Kremer, C.; Suescun, L.; Mombru, A.; Mariezcurrena, R.; Kremer, E. *Inorg. Chim. Acta* **2000**, *306*, 70−77. (j) Gable, K. P.; Khownium, K.; Chuawong, P. *Organometallics* **2004**, *23*, 5268−5274.
(12) Freedman, T. B.; Cao, X.; Dukor, R. K.; Nafie, L. A. *Chirality* **2003**, *15*, 743−758.
(13) (a) Holzwarth, G.; Hsu, E.; Mosher, H.; Faulkner, T.; Moscowitz, A. *J. Am. Chem. Soc.* **1974**, *96*, 251−2. (b) Nafie, L. A.; Cheng, J.; Stephens, P. *J. Am. Chem. Soc.* **1975**, *97*, 3842−3.
(14) (a) He, Y.; Cao, X.; Nafie, L. A.; Freedman, T. B. *J. Am. Chem. Soc.* **2001**, *123*, 11320−11321. (b) Freedman, T. B.; Cao, X.; Young, D. A.; Nafie, L. A. *J. Phys. Chem. A* **2002**, *106*, 3560−3565.

Scheme 1. Synthetic Route to the Four Oxorhenium(V) Complexes **4a** and **4b** Stereoisomers, Which Were Separated by Column Chromatography

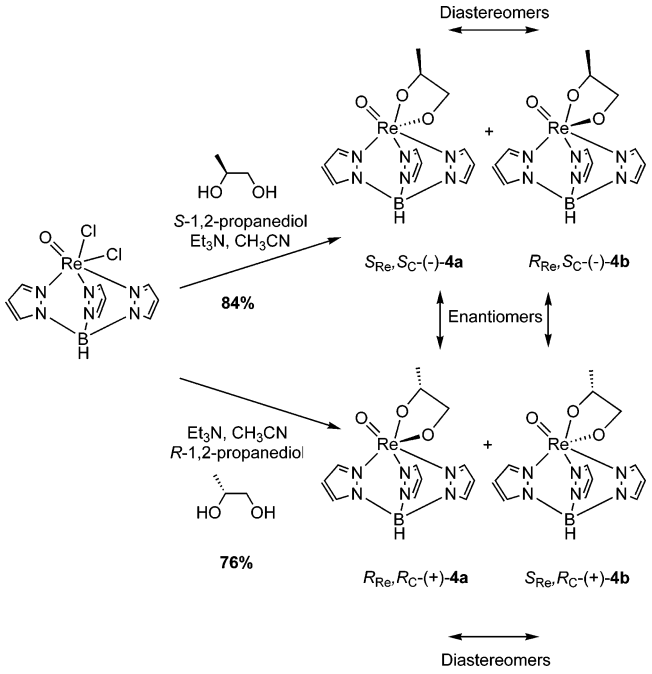

Scheme 2. Synthesis of Enantiomeric Oxorhenium Complexes **5** and **6** with the Use of Achiral Amino Alcohols

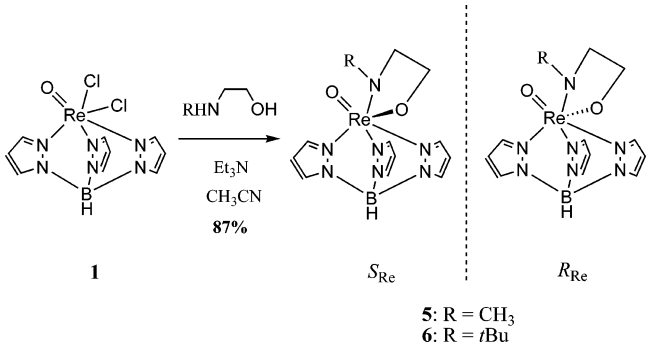

N,*O*)] (**2**) and (S_{Re},S_C)- and (R_{Re},R_C)-[TpReO(η^2-N(CH_2)$_3$-$CHCO_2$-*N*,*O*)] (**3**) because they were readily synthesized according to literature procedures[11b] from the precursor $TpReOCl_2$. For both cases, only one diastereomer was obtained among the two possible ones, due to steric interactions. The absolute configurations of these two compounds have already been determined by Faller and Lavoie by X-ray crystallography,[11b] and they could be confirmed by our VCD spectroscopy studies (see below). Following the same synthetic strategy, diastereomeric compounds (S_{Re},S_C)-**4a** and (R_{Re},S_C)-**4b** were obtained from (*S*)-1,2-propanediol as described in Scheme 1 together with their enantiomers (R_{Re},R_C)-**4a** and (S_{Re},R_C)-**4b** when using (*R*)-1,2-propanediol. No diastereoselectivity was observed with these less hindered chiral diols: the two possible diastereomers corresponding to both the *R* and *S* configurations at the rhenium chiral center were obtained in equal proportions. These diastereomers could however be separated by regular column chromatography over silical gel, and no epimerization was observed. (S_{Re},S_C)-(−)-**4a** and (R_{Re},S_C)-(−)-**4b** could therefore be obtained with ee's better than 99% from (*S*)-1,2-propanediol. Their enantiomers (R_{Re},R_C)-(+)-**4a** and (S_{Re},R_C)-(+)-**4b** could

Table 1. Crystallographic Data for Compounds **4a**, **4b**, and **5**

	(R_{Re},R_C)-(+)-**4a**	(R_{Re},S_C)-(−)-**4b**	**5**
empirical formula	$C_{12}H_{16}BN_6O_3Re$	$C_{12}H_{16}BN_6O_3Re$	$C_{12}H_{17}BN_7O_2Re$
fw	489.32	489.32	488.34
cryst syst	monoclinic	orthorhombic	monoclinic
space group	$P2_1$	$P2_12_12_1$	$P2_1/n$
unit cell dimensions	a = 8.3663(5) Å b = 8.3379(5) Å c = 11.3364(8) Å β = 101.869(3)°	a = 7.7937(4) Å b = 18.9861(10) Å c = 31.4245(17) Å	a = 10.4580(2) Å b = 10.6516(3) c = 14.5438(4) Å β = 96.703(1)°
unit cell vol (Å^3)	773.89(9)	4649.9(4)	1609.02(7)
Z	2	12	4
calcd density (g/cm^3)	2.100	2.097	2.016
abs coeff (mm^{-1})	7.874	7.863	7.572
F000	468	2808	936
cryst size (mm^3)	0.25 × 0.25 × 0.20	0.30 × 0.02 × 0.02	0.38 × 0.35 × 0.32
θ range for data collection (deg)	2.77−27.62	1.68−27.62	2.74−27.58
limiting indices	$-10 \le h \le +10$ $-10 \le k \le +9$ $-14 \le l \le +14$	$-10 \le h \le +9$ $-24 \le k \le +24$ $-40 \le l \le +40$	$-13 \le h \le +13$ $-13 \le k \le +13$ $-18 \le l \le +18$
no. of reflns collected/unique	5310/3344	58695/10698	28509/3691
R_{int}	0.034	0.045	0.040
completeness to θ_{max} (%)	96.7	99.3	99.1
transm coeff max/min	0.207/0.140	0.854/0.095	0.151/0.056
no. of data/ restraints/params	3344/1/028	10698/0/622	3691/0/208
GOF on F^2	1.105	0.995	1.058
final R indices [$I < 2\sigma(I)$], R1/wR2	0.0352/0.0891	0.0207/0.0340	0.0276/0.0685
final R indices (all data), R1/wR2	0.0392/0.0905	0.0261/0.0349	0.0335/0.073
absolute structure param	0.081(18)	−0.014(4)	
largest diff peak and hole (e·Å^{-3})	4.58/−2.41	0.68/−0.59	1.46/−1.90

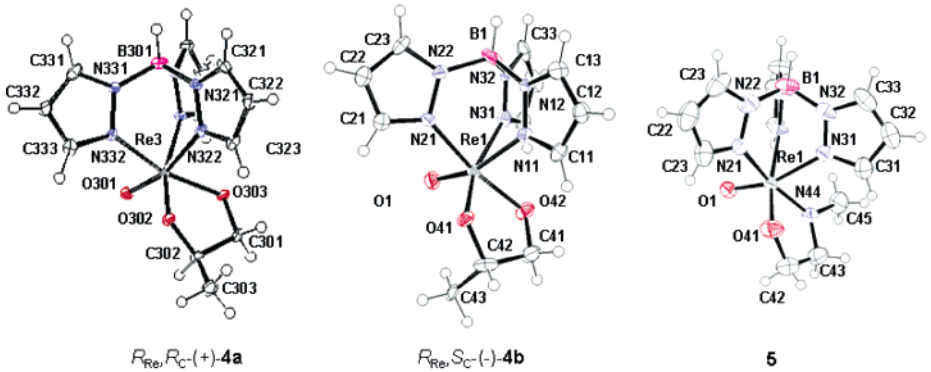

Figure 1. ORTEP diagrams (50% probability) of molecules (R_{Re},R_C)-(+)-**4a** and (R_{Re},S_C)-(−)-**4b** (only one out of three molecules in the asymmetric unit shown) and (±)-**5** (only one out of the two enantiomeric molecules in the asymmetric unit shown).

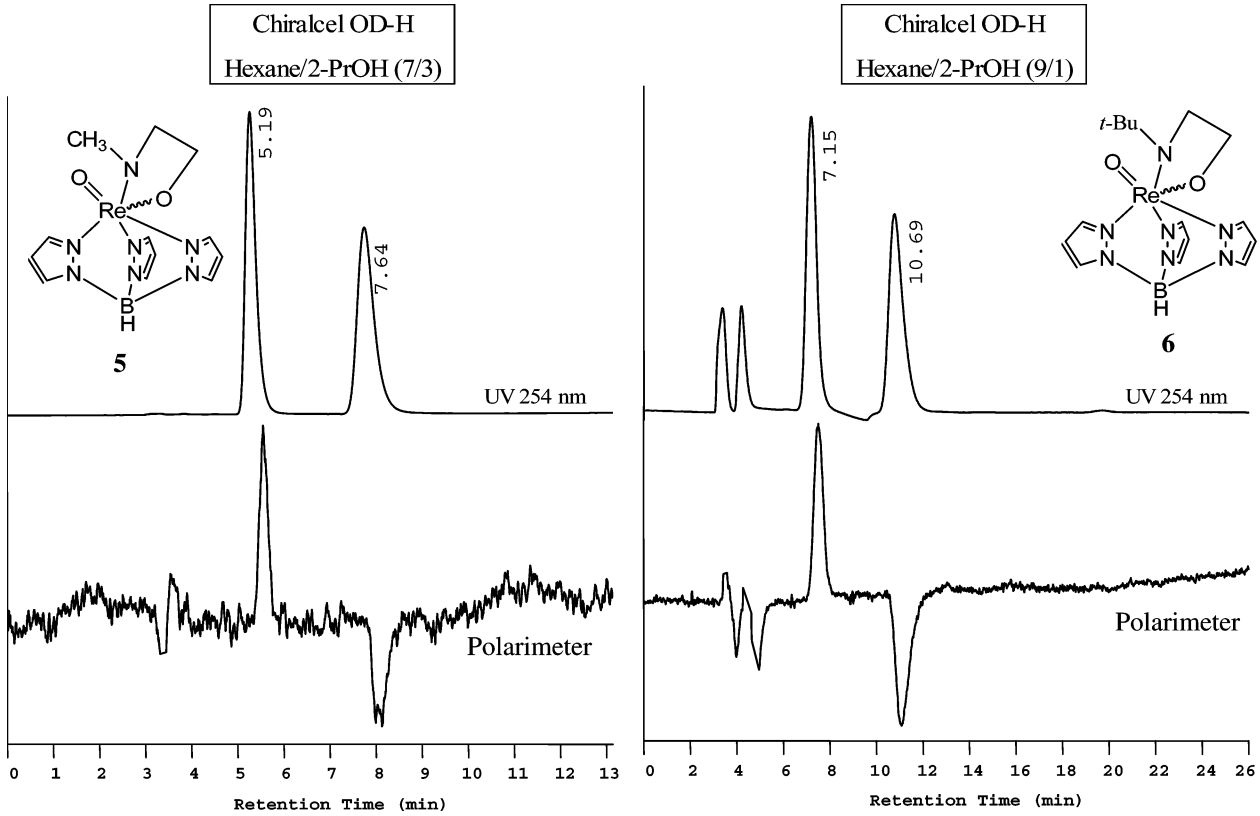

Figure 2. Analytical chiral HPLC chromatograms for the separations of compounds **5** and **6** on Chiralcel OD-H, with hexane/2-PrOH (7/3) as the mobile phase at 1 mL/min for **5** and hexane/2-PrOH (9/1) for **6** and with UV (254 nm) and polarimetric detectors.

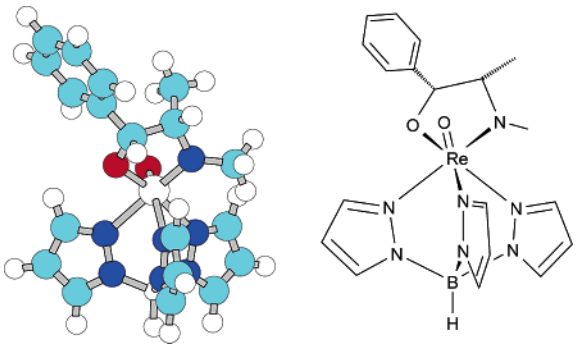

Figure 3. Optimized structure of the single conformer of (R_{Re},R_{O-C},S_{C-N})-**2**, **2-I** (B3LYP/6-31G(d)/Stuttgart calculation).

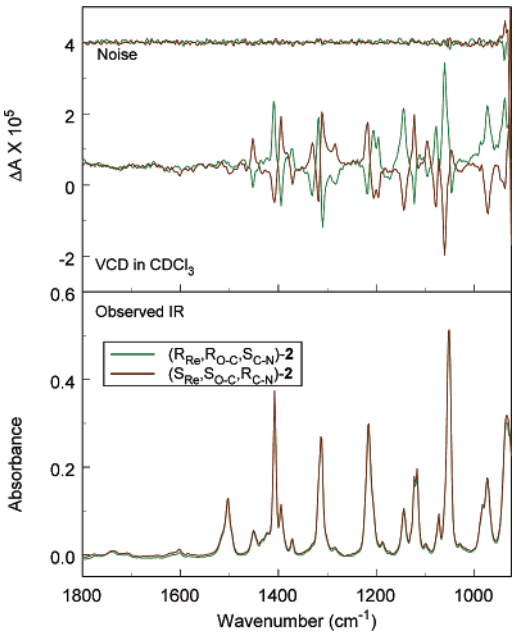

Figure 4. Observed IR (lower frame) and VCD (upper frame) of the two enantiomers of **2** in $CDCl_3$, 10 mg sample in 300 μL of solvent (58 mM), 4 cm^{-1} resolution, instrument optimized at 1400 cm^{-1}, collection time 12 h. IR spectra are solvent subtracted.

also be prepared in the same way by using (*R*)-1,2-propanediol. The absolute configurations (S_{Re},S_C)-(−) and (R_{Re},R_C)-(+) for **4a** and (R_{Re},S_C)-(−) and (S_{Re},R_C)-(+) for **4b** were first determined by VCD spectroscopy as explained in detail below. Later on, they were confirmed by X-ray crystallography analysis of (R_{Re},R_C)-(+)-**4a** and (R_{Re},S_C)-(−)-**4b** samples, which gave monocrystals and whose absolute structures are displayed in Figure 1. Their detailed crystallographic data are given in Table 1.

To simplify the molecules for PV experiments one step further enantiomerically pure pairs (R_{Re})- and (S_{Re})-**5** and (R_{Re})- and (S_{Re})-**6**, were prepared by using achiral amino alcohols, namely, *N*-methylaminoethanol and *N*-*tert*-butylaminoethanol. These compounds were prepared in their racemic form by reacting $TpReOCl_2$ with the achiral amino alcohols with good yields (Scheme 2). Monocrystals of (±)-**5** were obtained, and their X-ray structure analysis revealed a centrosymmetric space group, which means that the R_{Re} and S_{Re} enantiomers are found in the same asymmetric unit; i.e., (±)-**5** is a racemic compound (see Figure 1 and Table 1). The separation, impossible by direct crystallization, was therefore investigated by HPLC over chiral stationary phases.

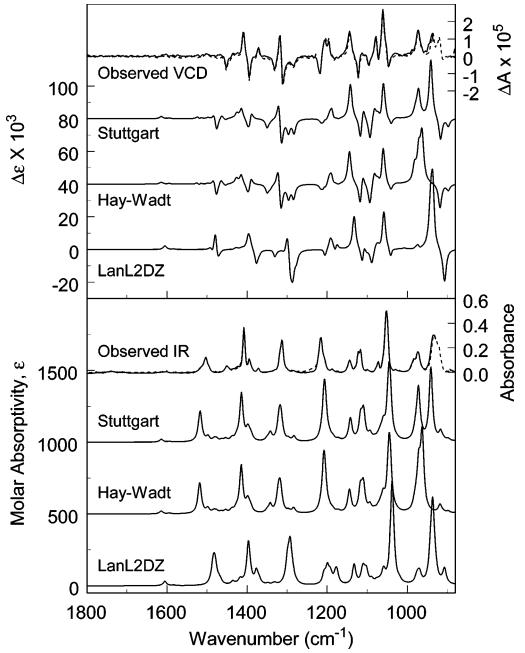

Figure 5. Observed IR (lower frame) and VCD (upper frame) spectra for (R_{Re},R_{O-C},S_{C-N})-**2** (right axes) compared to DFT calculations for **2-I** with the B3LYP functional and three basis sets (left axes, shown offset for clarity): LanL2DZ for all elements and Stuttgart or Hay−Wadt for Re with 6-31G(d) for elements H through O. Calculated frequencies are scaled by 0.97, and bandwidths are set to 5 cm^{-1}. Observed IR spectra are solvent subtracted, and VCD is baseline corrected using the average of the two enantiomers. Experimental data are presented for $CHCl_3$ solvent (dashed line) and $CDCl_3$ solvent (solid line). Experimental conditions are as in Figure 2.

The screening of CHIRBASE[15] revealed that a few chiral rhenium complexes have already been separated by this method.[16] Eleven chiral stationary phases were tested to find the best separation conditions to resolve the two enantiomers on a semipreparative scale (see the Supporting Information). For both racemates, Chiralcel OD-H (250 × 4.6 mm, cellulose tris-3,5-dimethylphenylcarbamate) gave excellent baseline separation and good enantioselectivity and resolution (see Figure 2). Therefore, the semipreparative chiral separations were performed on Chiralcel OD (250 × 10 mm) to give 22 mg of each enantiomer of **5** and 9 mg of each enantiomer of **6**, with enantiomeric excesses higher than 99.5% (see the Supporting Information for details). The separated enantiomers were characterized by their optical rotation: $[\alpha]_D^{25} = +935$ ($CHCl_3$, *c* 0.04) for the first eluted enantiomer of **5** and −930 ($CHCl_3$, *c* 0.04) for the second eluted enantiomer, $[\alpha]_D^{25} = +1240$ ($CHCl_3$, *c* 0.03) for the first eluted enantiomer of **6** and −1235 ($CHCl_3$, *c* 0.03) for the second eluted enantiomer. Those specific rotation values are the highest reported for such chiral rhenium compounds. Interestingly, samples of resolved **5** were heated at 50 °C in chloroform for 24 h, and no racemization could be observed. Furthermore, we have shown that compound **2** sublimates under mild conditions without alteration of its chemical composition and optical rotation. These features provide evidence for the robustness of these oxorhenium(V) compounds and allow confident consideration of the possibility to generate a molecular beam for high-resolution spectroscopy.

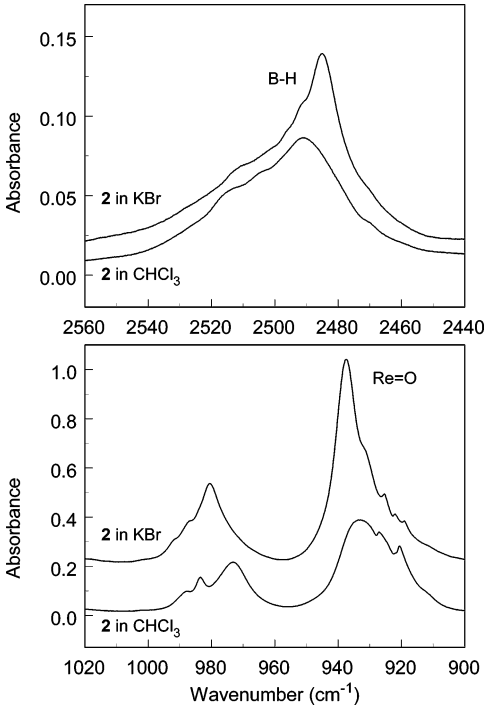

Figure 6. Higher resolution IR spectra of **2** in $CHCl_3$ solution and in a KBr pellet, showing the B−H stretching (top) and Re═O stretching (bottom) regions, resolution 0.25 cm^{-1}, collection time 90 min. KBr spectra are offset for clarity.

Oxorhenium complexes bearing a Cp* of the type $LReO_3$ have been extensively studied by Herrmann et al.[17] Replacement of the Tp ligand by a Cp* has been considered to simplify the structure of our complexes, and we have therefore synthesized [Cp*ReO(η^2-N(CH_3)CH(CH_3)CH(Ph)O-*N*,*O*)] from Cp^*ReOCl_2 and ephedrine, but we observed that such a complex was not stable at all and that epimerization at the rhenium center occurred spontaneously. We therefore did not pursue this direction further.

VCD Spectroscopy Studies. [TpReO(η^2-N(CH_3)CH(CH_3)CH(Ph)O-*N*,*O*)] (2). Conformational analysis revealed only one conformer of (R_{Re},R_{O-C},S_{C-N})-**2** (**2-I**), shown in Figure 3, optimized at the DFT/B3LYP level with the basis sets 6-31G(d) [H, B, C, N, O] and Stuttgart RSC 1997 ECP [Re][18] (abbreviated as 6-31G(d)/Stuttgart). Very little variation is seen in the optimized structure when different basis sets are used. Geometry optimization of the (S_{Re},R_{O-C},S_{C-N})-**2** diastereomer gave an energy 3.01 kcal/mol higher, suggesting a population fraction of 0.6%, consistent with the results from the synthesis.

(15) Roussel, C.; Piras, P. CHIRBASE. http://chirbase.u-3mrs.fr, database of current status and derived research applications using molecular similarity, a decision tree, and a 3D "enantiophore" search, pp 95−125. Roussel, C.; Pierrot-Sanders, J.; Heitmann, I.; Piras, P. In *Chiral Separation Techniques—A Practical Approach*, 2nd completely revised and updated ed.; Subramanian, G., Ed.; Wiley-VCH: Weinheim, Germany, 2001.

(16) (a) Ramsden, J. A.; Garner, C. M.; Gladysz, J. A. *Organometallics* **1991**, *10*, 1631−1633. (b) Green, J. M.; Jones, R.; Harrison, R. D.; Edwards, D. S.; Glajch, J. L. *J. Chromatogr.* **1993**, *635*, 203−209. (c) Ciruelos, S.; Englert, U.; Salzer, A.; Bolm, C.; Maischak, A. *Organometallics* **2000**, *19*, 2240−2242.

(17) Romao, C. C.; Kuhn, F. E.; Herrmann, W. A. *Chem. Rev.* **1997**, *97*, 3197−3246.

(18) Andrae, D.; Haussermann, U.; Dolg, M.; Stoll, H.; Preuss, H. *Theor. Chim. Acta* **1990**, *77*, 123−41.

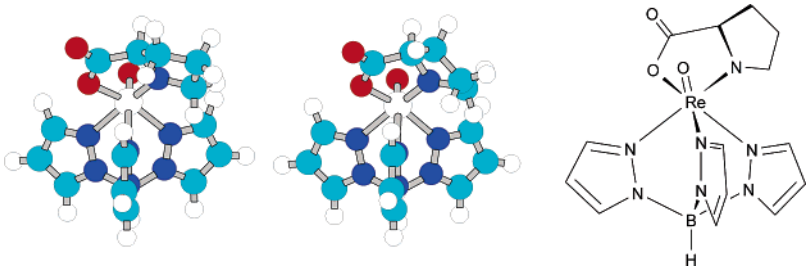

Figure 7. Two optimized conformers of (R_{Re},R_C)-**3**, **3-I** (left, 51%) and **3-II** (center, 49%). Geometries were optimized using B3LYP/6-31G(d)/Stuttgart.

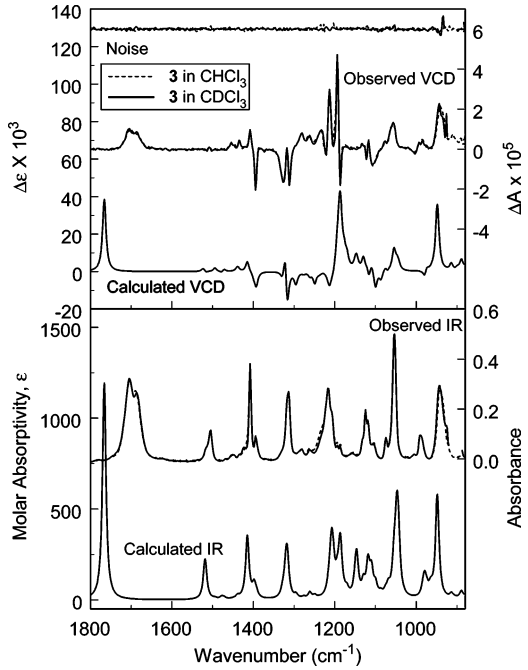

Figure 8. Expeimental IR (bottom) and VCD (top) spectra for (−)-**3**, with VCD noise as the uppermost trace (right axes, both chloroform and deuterated chloroform solutions, 5 mg/150 μL of solvent (63 mM), IR spectra solvent subtracted, VCD spectra enantiomer subtracted, 4 cm^{-1} resolution, instrument optimized at 1400 cm^{-1}, collection time 12 h) compared to calculated spectra for (R_{Re},R_C)-**3** (left axes, B3LYP/6-31G(d)/Stuttgart, frequencies scaled by 0.97, bandwidth set to 5 cm^{-1}) averaged for the two conformers **3-I** and **3-II**.

IR and VCD spectra of **2** are shown in Figure 4, where the IR and raw VCD spectra of both enantiomers in $CDCl_3$ are shown. The VCD intensities are very close to opposite in sign for the enantiomers. Because both enantiomers were available for this study, to eliminate minor absorption artifacts and increase the signal-to-noise ratio compared to use of a solvent baseline, the average VCD spectrum of the enantiomers (corresponding to a racemic sample) was used as the VCD baseline in subsequent figures.

In Figure 5, the observed IR and VCD spectra are compared to the array of calculated ones with the B3LYP functional and the basis set LanL2DZ for all elements[19−21] or a combination of 6-31G(d) for elements H through O and a larger basis set for Re (Hay−Wadt VDZ (n+1) ECP[22] or Stuttgart RSC 1997 ECP.[18] Experimental spectra using both $CHCl_3$ and $CDCl_3$ solutions have been combined to cover a wider spectral range to 880 cm^{-1}. A progressively better fit to the experimental spectra can be seen when the basis set size is increased. The results for the SDD basis set for all elements (not shown) are almost identical to the B3LYP/LanL2DZ calculation. In general, the comparison of observed and calculated VCD spectral patterns is quite good and allows for an unambiguous verification of the absolute configuration. However, the relative intensities of VCD peaks differ somewhat between the observed and calculated spectra. We find the best agreement using the combination of the Stuttgart basis set for rhenium and 6-31G(d) for the other elements.

Most of the observed vibrational bands can be assigned on the basis of the Gaussian 03 calculations. The Re═O stretching band at ∼930 cm^{-1} is the most interesting vibration in this study because of the ongoing search for PV effects. The two large basis sets for rhenium yield slightly different results in the Re═O stretching region. With the Hay−Wadt basis set for Re, the Re═O stretch couples more strongly with a phenyl ring deformation than with the Stuttgart basis set (which has an additional 15 basis functions). In addition to the large Re═O stretching motion, the normal mode generating a positive VCD intensity for **2** at ∼930 cm^{-1} has contributions from deformations of the entire ephedrine ligand, as well as Tp deformation.

Closer inspection of the observed Re═O stretching band reveals a non-Lorentzian shape due to shoulders at lower frequencies, which are not readily assigned by the calculations. Similarly, the B−H stretching band at 2500 cm^{-1} has shoulders at higher frequencies. Figure 6 displays higher resolution (0.25 cm^{-1}) IR spectra in these regions, recorded for samples both in $CHCl_3$ solution and as a KBr pellet. The shoulders cannot be readily assigned to other normal modes, since there is only one additional calculated normal mode near the Re═O stretch, and its calculated IR intensity is 2 orders of magnitude smaller. The B−H stretching band is completely isolated between the fingerprint and C−H stretching regions.

Several explanations can be invoked to explain the observed shoulders. Both rhenium and boron have naturally occurring isotopes, i.e., 37% ^{185}Re and 20% ^{10}B, which would generate minor peaks at shifted frequencies. The size of these frequency shifts can be estimated from the reduced masses or calculated for the isotope with Gaussian 03 to be 0.37

(19) Dunning, T. H., Jr.; Hay, P. J. In *Modern Theoretical Chemistry*; Schaefer, H. F., III, Ed.; Plenum: New York, 1976; Vol. 3, pp 1−28.
(20) Hay, P. J.; Wadt, W. R. *J. Chem. Phys.* **1985**, *82*, 299−310.
(21) Wadt, W. R.; Hay, P. J. *J. Chem. Phys.* **1985**, *82*, 284−98.
(22) Hay, P.; Wadt, W. *J. Chem. Phys.* **1985**, *82*, 299−310.

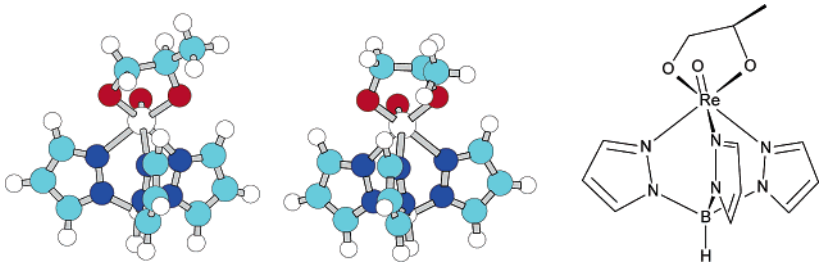

Figure 9. Two conformers of (R_C,R_{Re})-**4a**, **4a-I** (left, 97%) and **4a-II** (center, 3%), optimized using B3LYP/6-31G(d)/Stuttgart.

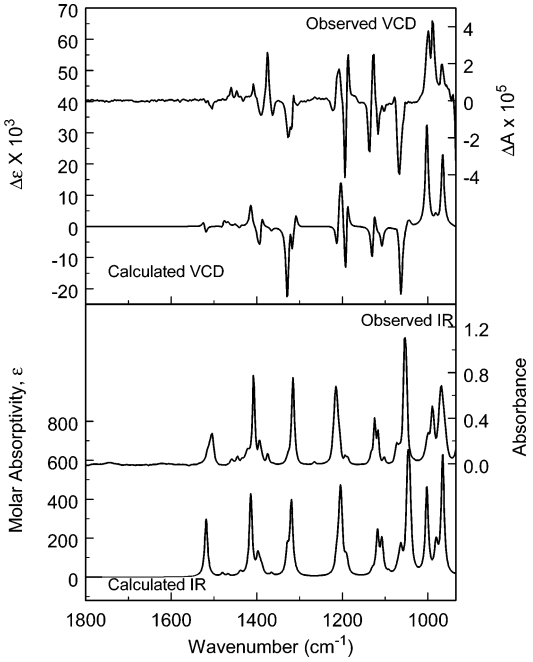

Figure 10. IR (bottom) and VCD (top) spectra for (R_C,R_{Re})-**4a**. Calculated spectra (left axis) are weighted averages of the two conformers, 87% **4a-I** + 13% **4a-II**, determined using B3LYP/6-31G(d)/Stuttgart. Frequencies are scaled by 0.97, and the bandwidth is set to 4 cm^{-1}. Observed spectra for (−)-**4b** (right axis, 4 mg/100 μL of $CDCl_3$ (81 mM)) are solvent subtracted, resolution 4 cm^{-1}, instrument optimized at 1400 cm^{-1}, collection time 9 h.

cm^{-1} for Re═O and 11 cm^{-1} for B−H, making only the B−H shift observable experimentally. Additional shoulders in the B−H stretching region may arise from Fermi resonance with overtones of B−H deformations, which indeed are found in the calculation at around half the stretching frequency. The shoulders to the Re═O stretch may also arise due to Fermi resonance, since the calculated Re═O stretching at 970 cm^{-1} (unscaled) matches combination bands for modes calculated at 146 and 823 cm^{-1} (involving the N−Re═O angle deformation), as well as 301 and 669 cm^{-1} (involving ephedrine chelate ring deformation).

IR spectra at a roughly 13 times lower concentration were recorded, and they reveal practically no difference in band shape beyond the scaling factor (data not shown). This evidence supports the possibility of solvent interaction or intramolecular effects such as Fermi resonance and precludes solute−solute interactions as sources for the additional weak features in the B−H and Re═O stretching regions.

[TpReO(η^2-N(CH_2)$_3$$CHCO_2$-*N*,*O*)] (3). Two conformers of the (R_{Re},R_C)-[TpReO(η^2-N(CH_2)$_3$$CHCO_2$-*N*,*O*)] sample (**3**) have been identified, with different puckering of the five-membered proline ring, referred to as **3-I** and **3-II**, shown in Figure 7. In the gas phase, the calculated energies for the two conformers differ by 0.11 kcal/mol according to the B3LYP/LanL2DZ calculation, corresponding to Boltzmann populations of 55% **3-I** vs 45% **3-II**. With the 6-31G(d)/Stuttgart basis set, the energy difference is smaller and opposite, with **3-I** lying 0.013 kcal/mol higher in energy, suggesting almost equal populations. Interestingly, the presence of two conformers is also suggested by the published crystal structure,[11b] where the relevant 50% probability ellipsoids in the ORTEP representation appear prolate. At the B3LYP/LanL2DZ level, the (S_{Re},R_C)-**3** diastereomer is calculated to lie 5.1 kcal/mol higher in energy than (R_{Re},R_C)-**3**, consistent with the presence of only the R_{Re},R_C diastereomer in the experimental sample.

IR and VCD spectra were calculated for both conformers **3-I** and **3-II**, and the average spectra for the two conformers (B3LYP/6-31G(d)/Stuttgart) are compared to experiment in Figure 8. The overall agreement in VCD patterns between the observed and calculated spectra again provides an unambiguous assignment of absolute configuration, but the agreement is not as good as for **2**. A positive VCD intensity near 1200 cm^{-1} correlates with modes involving the proline ligand. The carbonyl stretching mode is calculated to exhibit fairly intense, positive VCD intensity, but with a frequency 100 cm^{-1} too high with 6-31G(d)/Stuttgart and 100 cm^{-1} too low with LanL2DZ and SDD basis sets (not shown).

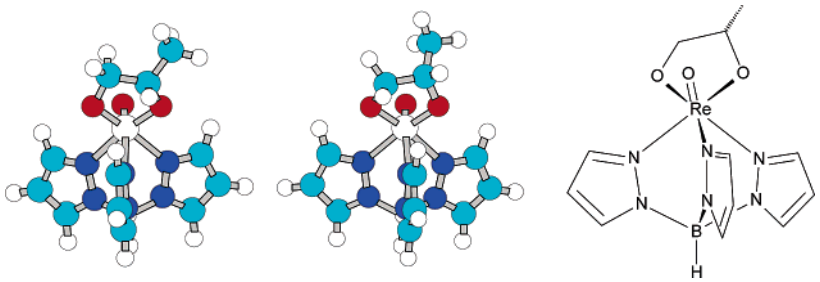

Figure 11. Two conformers of (S_C,R_{Re})-**4b**, **4b-I** (left, 87%) and **4b-II** (center, 13%), optimized using B3LYP/6-31G(d)/Stuttgart.

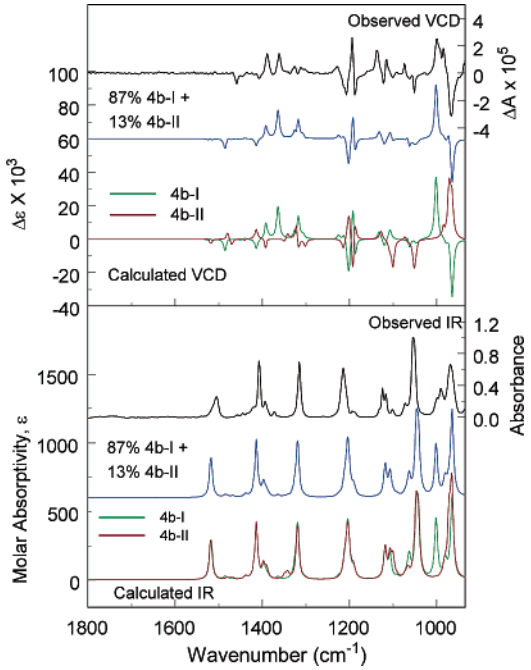

Figure 12. IR (bottom) and VCD (top) spectra for (S_C,R_{Re})-**4b**. Calculated spectra (left axis) are weighted averages of the two conformers **4b-I** and **4b-II** determined using B3LYP/6-31G(d)/Stuttgart. Frequencies are scaled by 0.97, and the bandwidth is set to 4 cm^{-1}. Observed spectra for (−)-**4b** (right axes, 4 mg/100 μL of $CDCl_3$ (81 mM)) are solvent subtracted, resolution 4 cm^{-1}, instrument optimized at 1400 cm^{-1}, collection time 9 h.

The observed C═O stretching band also has two separate peaks observed at 1691 and 1704 cm^{-1}, but the calculated carbonyl stretching frequencies for the two conformers differ only by 2 cm^{-1}. The Re═O and B−H bands also reveal shoulders in the 0.25 cm^{-1} resolution IR spectra (data not shown), which can be explained in the same way as for **2**.

[TpReO(η^2-O(CH_3)CH_2CH_2O-*O*,*O*)] (4a and 4b). For the diastereomer (R_{Re},R_C)-**4a**, two diolate conformers were identified at the B3LYP/6-31G(d)/Stuttgart level that differ by 2.2 kcal/mol, suggesting only a 3% population of the minor conformer (R_{Re},R_C)-**4a-II** (Figure 9). The comparison between the composite calculated spectra and the observed spectrum for (+)-**4a**, shown in Figure 10, provides an unambiguous assignment of absolute configuration for this experimental diastereomer sample fraction as (R_{Re},R_C)-(+)-**4a**, consistent with the X-ray crystallography analysis presented above. The Re═O stretch, calculated at 965 cm^{-1} (scaled by 0.97), correlates with a positive VCD band at 966 cm^{-1}.

Two optimized conformers that differ in conformation of the chelated diolate ring were identified for the diastereomer (R_{Re},S_C)-**4b** at the B3LYP/6-31G(d)/Stuttgart level, shown in Figure 11. Conformer **4b-II** is higher in energy by 1.1 kcal/mol, yielding a population of 87% **4b-I** and 13% **4b-II** at room temperature. The calculated conformer spectra and their Boltzmann-population-weighted composite are compared to experiment for (−)-**4b** in Figure 12, demonstrating very good agreement in VCD pattern and identifying the absolute configuration of this sample as (R_{Re},S_C)-(−)-**4b**. In this case, the band with a predominant Re═O stretch at 965 cm^{-1} (scaled frequency) has opposite signs for the two conformers and correlates with the negative VCD at 968 cm^{-1}, consistent with the larger population of **4b-I**. The comparison between the observed and calculated spectra for the two conformers provides evidence for the presence of both conformers in solution, where, for example, the negative feature at 1050 cm^{-1} is characteristic of the minor conformer and the positive VCD feature at 1000 cm^{-1} is characteristic of the major conformer.

[TpReO(η^2-N(CH_3)CH_2CH_2O-*N*,*O*)] (5). The chelated bidentate ligand can assume two conformers, calculated to differ in energy by 0.30 kcal/mol, with populations of 62% **5-I** and 38% **5-II** (Figure 13). From the Boltzmann-population-weighted sum of the calculated spectra, shown in Figure 14, sufficient agreement with experiment is found for assignment of the absolute configuration as (R_{Re})-(−)-[TpReO(η^2-N(CH_3)CH_2CH_2O-*N*,*O*)]. In regions where the two conformers exhibit VCD bands opposite in sign, the agreement between the composite calculated spectra and experiment is not quite as good. The Re═O stretches for the two conformers are opposite in sign, with a rather weak negative VCD intensity calculated for the dominant conformer at 945 cm^{-1} (scaled frequency). An absorption band near this frequency appears at the cutoff for the $CDCl_3$ solvent measurements, but no distinct VCD feature is observed for **5** in this region.

[TpReO(η^2-N(*t*Bu)CH_2CH_2O-*N*,*O*)] (6). The two optimized conformers for **6**, shown in Figure 15, differ by 2.5 kcal/mol, indicating a population of less than 2% for conformer **6-II**. The comparison of the experimental VCD spectrum for (−)-**6** with the calculated spectrum for **6-I** (Figure 16) identifies the absolute configuration as (R_{Re})-(−)-[TpReO(η^2-N(*t*Bu)CH_2CH_2O-*N*,*O*)]. The Re═O stretch generates the positive VCD band at ∼940 cm^{-1}.

Summary

We have recorded good-quality IR and VCD spectra of six enantiomeric pairs of rhenium complexes and successfully verified their absolute configuration by comparison to spectra

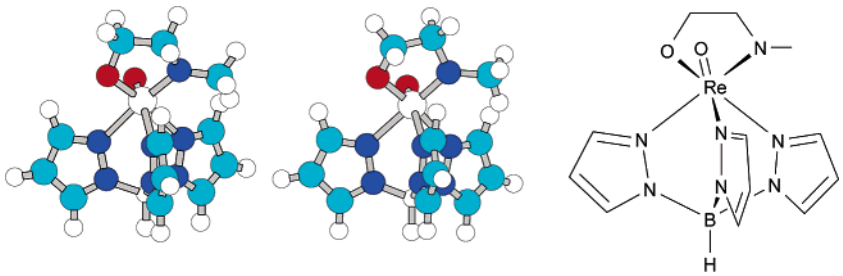

Figure 13. Two conformers of (R_{Re})-**5**, **5-I** (left, 62%) and **5-II** (right, 38%), optimized using B3LYP/6-31G*/Stuttgart.

Table 2. Summary of Results for VCD Analysis

	2	3	4a	4b	5	6
absolute config	(R_{Re},R_{O-C},S_{C-N})-(+)	(R_{Re},R_C)-(-)	(R_{Re},R_C)-(+)	(R_{Re},S_C)-(−)	(R_{Re})-(−)	(R_{Re})-(−)
mol wt	578.452	528.349	489.312	489.312	488.327	530.408
calcd conformer populations (23 °C)	100% **2-I**	51% **3-I**	97% **4a-I**	89% (**4b-I**)	62% **5-I**	98% **6-I**
		49% **3-II**	3% **4a-II**	13% **4b-II**	38% **5-II**	2% **6-II**
calcd Re═O stretch (cm^{-1}) scaled by 0.97 and VCD rotational strengths[a]	941 (+141)	949 (**3-I**) (+120)	965 (**4a-I**) (+68)	965 (**4b-I**) (−107)	946 (**5-I**) (−11)	940 (**6-I**) (+124)
		946 (**3-II**) (+158)	963 (**4a-II**) (−129)	965 (**4b-II**) (+64)	944 (**5-II**) (+75)	942 (**6-II**) (+48)
obsd Re═O stretch (cm^{-1}) and VCD sign	934 (+)	943 (+)	966 (+)	965 (−)	not obsd	940 (+)

[a] Calculated rotational strength for the Re═O stretch, 10^{-44} esu^2 cm^2.

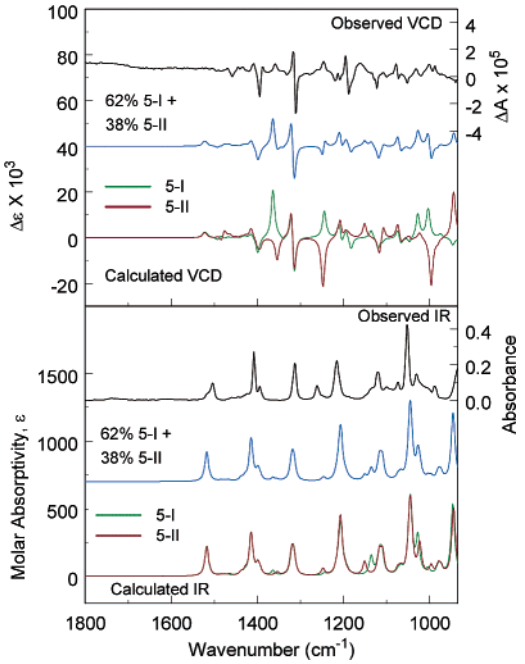

Figure 14. IR (bottom) and VCD (top) spectra for (R_{Re})-**5**. Calculated spectra of the two conformers **5-I** and **5-II** and their Boltzmann-population-weighted sum (left axes, B3LYP/6-31G(d)/Stuttgart, frequencies scaled by 0.97, bandwidth 5 cm^{-1}) are compared to observed spectra for (−)-**5** (right axes, 3 mg/100 μL of $CDCl_3$ (61 mM), solvent subtracted, resolution 4 cm^{-1}, instrument optimized at 1400 cm^{-1}, collection time 12 h).

calculated at the DFT level for one of each enantiomeric pair. Several basis sets have been investigated, and the best fit to experiments has been obtained using the B3LYP functional and a custom basis set for rhenium, Stuttgart RSC 1997 ECP, along with 6-31G(d) for the remaining elements.

Only one conformer of **2** was found during the calculations, but the remaining samples exist in solution as two chelate ring conformers with different populations. For **3**, **4b**, and **5**, both conformers contribute to the observed spectra in solution at room temperature. The differences in energy for the chelate ring conformers arise primarily from steric effects. Including solvent in the calculations would probably have only minor effects on the calculated solution populations. Adjusting the relative populations for the conformers of **3**, **4b**, and **5** did not improve the fit to experiment compared to the calculated Boltzmann populations. The Re═O stretch is identified by a distinct VCD band in the 930−965 cm^{-1} region in **2**, **3**, **4a**, **4b**, and **6**. For **5**, the opposite signs for the VCD of the two populated conformers result in little or no VCD intensity for the Re═O stretch.

All samples investigated reveal some bands with several components, both in solution and in a solid-state matrix. This is apparent from the fine structure of the Re═O stretch and B−H stretching absorption bands, which consist of several peaks, and most prominently from the C═O vibration of **3**, which has two distinct peaks. Both inter- and intramolecular effects have been considered to explain these effects. In solution, we expect negligible solvent interaction. We attribute the splitting of the B−H and Re═O stretching bands to a Fermi resonance and isotope shifts by ^{10}B. The key results for all the samples have been summarized in Table 2.

Conclusion

New chiral oxorhenium(V) complexes have been synthesized from $TpReOCl_2$ and suitable chiral diols or achiral amino alcohols. Regular column chromatography could be used to prepare diastereomerically pure complexes [TpReO(η^2-O(CH_3)CH_2CH_2O-*O*,*O*)] [(S_{Re},S_C)-(−)-**4a** and (R_{Re},S_C)-(−)-**4b** and their mirror images]. On the other hand, semipreparative HPLC over chiral stationary phases has proven very efficient to obtain enantiomerically pure complexes [TpReO(η^2-N(CH_3)CH_2CH_2O-*N*,*O*)] [(S_{Re})-(+)- and (R_{Re})-(−)-**5**] and [TpReO(η^2-N(*t*Bu)CH_2CH_2O-*N*,*O*)] [(S_{Re})-(+)- and (R_{Re})-(−)-**6**]. Absolute configurations were determined by VCD studies, and some were confirmed by X-ray crystallography. The advantages vs drawbacks of using such

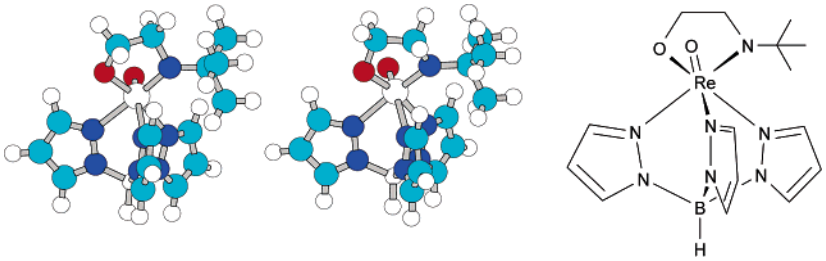

Figure 15. Two conformers of (R_{Re})-**6**, **6-I** (left, 98%) and **6-II** (center, 2%), optimized using B3LYP/6-31G(d)/Stuttgart.

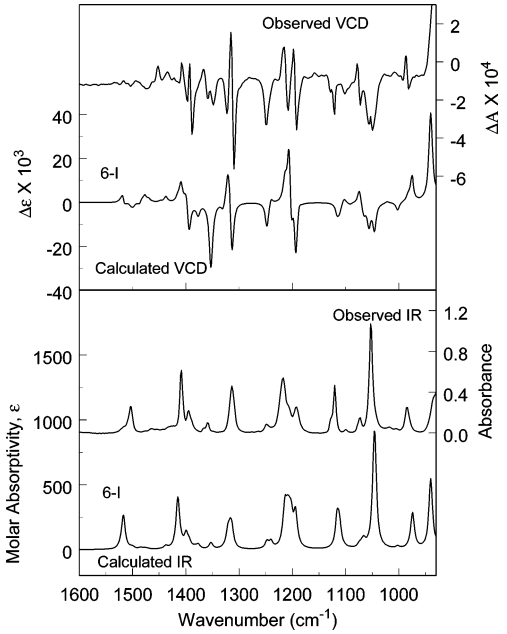

Figure 16. IR (bottom) and VCD (top) spectra for (R_{Re})-**6**. Calculated spectra of the predominant conformer **6-I** (left axis, B3LYP/6-31G(d)/Stuttgart, frequencies scaled by 0.97, bandwidth 4 cm^{-1}) are compared to observed spectra for (−)-**6** (right axis, 4.8 mg/100 μL of $CDCl_3$, solvent subtracted, resolution 4 cm^{-1}, instrument optimized at 1400 cm^{-1}, collection time is 12 h).

chiral complexes for parity violation experiments have been considered. The main advantages are their ease of synthesis, their robustness, and their enantiomeric stability, which is not straightforward in inorganic chemistry. These complexes all display a sharp Re═O stretching mode that may be carefully studied by using an ultrastable CO_2 laser in the case of ultra-high-resolution IR spectroscopy.[7] The main drawbacks are the total number of atoms (especially because of the Tp ligand) and the presence of several conformational isomers in solution as evidenced by VCD. Indeed, in addition to identification of the absolute configuration of the complexes without the need for X-ray studies, the VCD study has characterized the solution conformers of the complexes and identified complexes that may not be suitable for further study because of opposite VCD intensities (and presumably other chiral properties) for the Re═O stretch for two populated conformers (**4b** and **5**). The Re═O stretches are identified by distinct vibrational bands in the region 930−965 cm^{-1}, with dominant Re═O stretching motion accompanied by motion of the ligand rings. The sign and intensity of the Re═O stretching VCD are influenced by the chirality at the rhenium, the chirality of the ligand chelating TpReO, and the conformation of the chelating ligand.

Acknowledgment. The Agence Nationale pour la Recherche (ANR) is warmly thanked for funding (NCPMOL project).

Supporting Information Available: Listings of experimental procedures, HPLC separations, crystallographic data, VCD measurements, and theoretical calculations. This material is available free of charge via the Internet at http://pubs.acs.org.

IC061418M